

Communication

Synthesis and Characterization of Novel Indazole–Sulfonamide Compounds with Potential MAPK1 Inhibitory Activity for Cancer Treatment

Nassima Saghdani, Abdelali Chihab , Nabil El Brahmi  and Saïd El Kazzouli * 

Euromed Research Center, Euromed Faculty of Pharmacy, School of Engineering in Biomedical and Biotechnology, Euromed University of Fes (UEMF), Fez 30000, Morocco; nassima.saghdani@femg.ueuromed.org (N.S.); a.chihab@biomedtech.ueuromed.org (A.C.); n.elbrahmi@ueuromed.org (N.E.B.)

* Correspondence: s.elkazzouli@ueuromed.org

Abstract: Indazoles are a very important group of nitrogen-containing heterocycles with a wide range of biological and medicinal applications. These properties make them highly attractive for drug development, particularly when combined with sulfonamides to enhance their medicinal potential. In this work, we synthesized an indazole-based sulfonamide, namely the 1-((2-chloro-5-methoxyphenyl)sulfonyl)-5-nitro-1*H*-indazole (**3**). The reduction of the nitro group of 5-nitroindazole (**1**) to its corresponding amine was also performed to yield compound (**4**). Both compounds' structures were elucidated using various spectroscopic techniques such as ¹H NMR, ¹³C NMR, infrared (IR), and high-resolution mass spectrometry (HRMS). Our molecular docking studies suggest that compounds (**3**) and (**4**) have a strong affinity for MAPK1, indicating their potential as cancer treatments.

Keywords: indazole; sulfonamides; sulfonylation reaction; MAPK1; molecular docking



Citation: Saghdani, N.; Chihab, A.; El Brahmi, N.; El Kazzouli, S. Synthesis and Characterization of Novel Indazole–Sulfonamide Compounds with Potential MAPK1 Inhibitory Activity for Cancer Treatment. *Molbank* **2024**, *2024*, M1858. <https://doi.org/10.3390/M1858>

Academic Editor: Fawaz Aldabbagh

Received: 9 July 2024

Revised: 18 July 2024

Accepted: 22 July 2024

Published: 26 July 2024



Copyright: © 2024 by the authors. Licensee MDPI, Basel, Switzerland. This article is an open access article distributed under the terms and conditions of the Creative Commons Attribution (CC BY) license (<https://creativecommons.org/licenses/by/4.0/>).

1. Introduction

N-heterocyclic compounds possess unique structural units and widely exist in the bioactive molecules and natural products [1–5]. Among these, indazoles exhibit a large spectrum of pharmacological activities [6,7] including anti-cancer, anti-bacterial, anti-inflammatory, anti-depressant, and anti-hypertensive activities [8–13]. Cancer treatment has progressed significantly. Currently, at least 43 indazole-based drugs are in clinical trials or have been approved for use [14,15]. In addition, sulfonamides also are among the first important therapeutic agents widely used in the treatment of several diseases. Any molecule whose structure includes a section (SO₂NH₂) is called a sulfonamide. These compounds have gained significant consideration due to their various biological processes in the agricultural and pharmaceutical fields [16,17]. In its capacity as a bioisostere for the carboxylic group, the sulfonamide moiety possesses the inherent advantage of circumventing several limitations associated with carboxylic groups, notably including issues of metabolic instability, toxicity, and constrained passive diffusion across biological membranes [18]. Sulfonamide moieties have been consistently identified within a diverse range of pharmaceuticals, biomolecules, and biologically active compounds, showcasing an extensive array of biological functionalities. These functionalities encompass anti-fungal effects [19], anti-inflammatory properties [20], antibacterial [21], antiviral [22], anti-HIV drugs [23], and anti-cancer activities [24,25]. Here we report the synthesis of new indazole–sulfonamide derivatives and their molecular docking against the MAPK1 target.

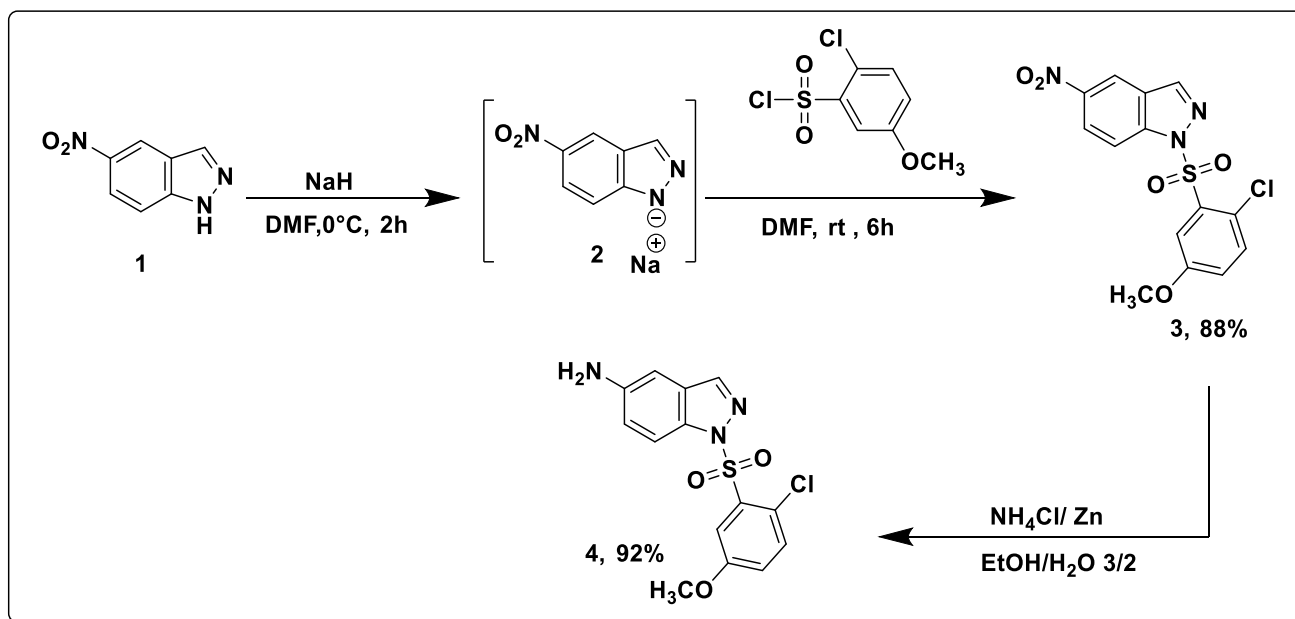
2. Results

2.1. Synthesis

Initially, commercially available 5-nitroindazole (**1**) was dissolved in dry *N,N*-dimethylformamide (DMF) at 0 °C. Then it was reacted with sodium hydride (NaH). This resulted

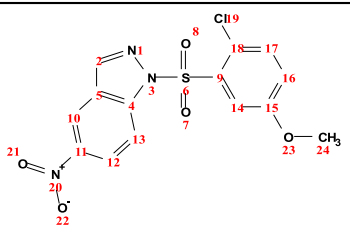
in the formation of the corresponding sodium salt of 5-nitro-1*H*-indazole (2) as an intermediate, accompanied by the release of hydrogen gas. The mixture was stirred for 30 min and eventually 2-chloro-5-methoxybenzene-1-sulfonyl was added. Then, the reaction proceeded at room temperature for 6 h to give exclusively compound (3) as the N1 isomer.

Afterward, compound (3) underwent a reduction reaction in a mixture of EtOH and H₂O as solvents. Then ammonium chloride (NH₄Cl) was added followed by zinc after a 5 min incubation period, the mixture was stirred for 3 h at room temperature to give compound (4) in a very good yield as illustrated in Scheme 1. Finally, the compounds (3) and (4) were purified using column chromatography and characterized with ¹H NMR, ¹³C NMR, IR, and HRMS.

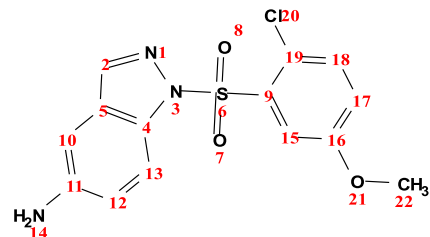


Scheme 1. Synthesis of compounds (3) and (4).

The ¹H NMR spectrum of compound (3) indicates that the aromatic protons from both the indazole and phenyl rings exhibit signals between 6.82–8.9 ppm. The methoxy group (OCH₃) appears at 3.44 ppm as singlet signal integrating for three protons (Figure 1 and Table 1). In order to determine whether sulfonylation occurred at the N1 or N2 position of indazole, NOESY NMR experiment was realized. As shown in Figure 2, the proton at position three of indazole does not show any spatial correlations with other protons. This lack of correlation indicates that the aromatic protons of the sulfonamide part are not in close proximity to the proton at position three, confirming that the reaction occurred at the N1 position of indazole. The reduction of the nitro group of (3) into its amine analog was confirmed by the ¹H NMR. The spectrum of compound (4) shows the presence of broad singlet integrating for two protons appearing at around 5.22 ppm which is attributed to the amine group (NH₂). Furthermore, a slight upfield shift (lower ppm values) as observed for the aromatic protons of compound (4) which appear in the range of 6.72–8.17 ppm, further confirming this transformation. This upfield shift was also observed for the methoxy group of (4) which appears as a singlet near 3.35 ppm (Figure 3 and Table 2).

Table 1. Complete ^1H NMR and ^{13}C NMR signal assignments for compound (3).


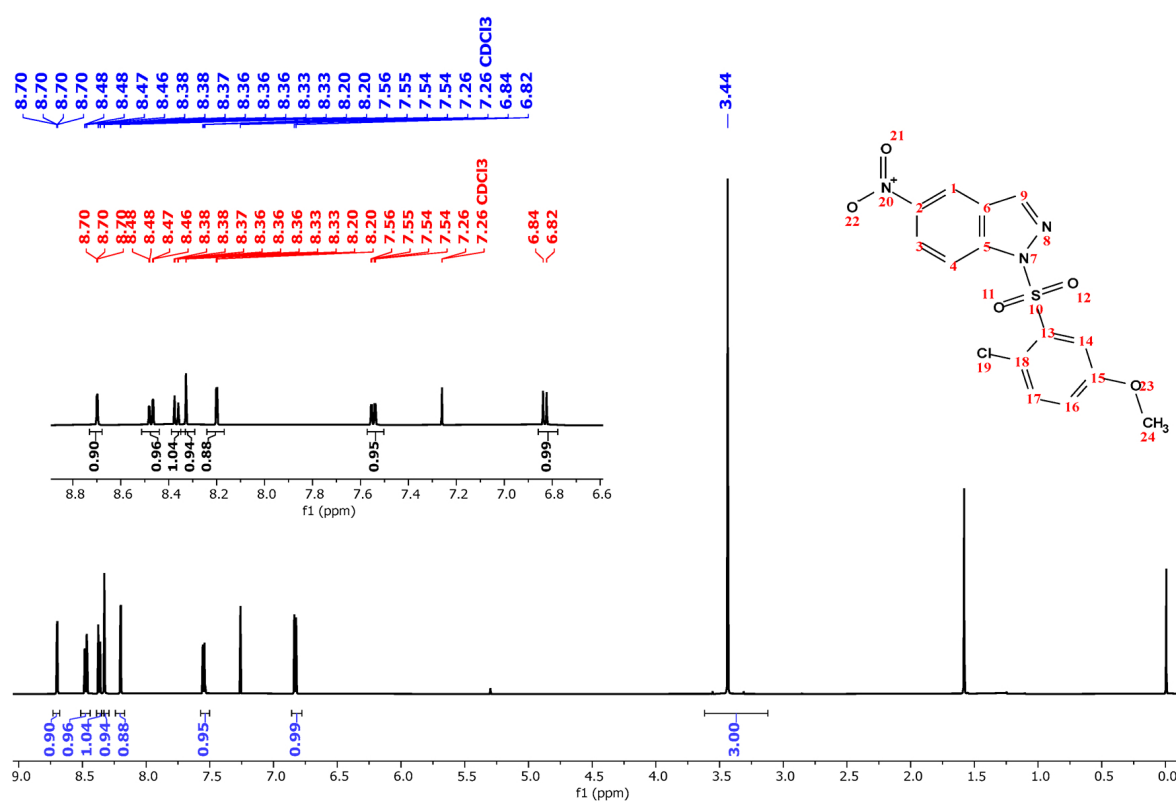
δ (ppm)	Integration	Multiplicity	Coupling Constant (Hz)	Assignment
3.44	3	s	—	3H (24)
6.83	1	d	8.9	H (17)
7.55	1	dd	8.9, 2.6	H (16)
8.20	1	d	2.2	H (14)
8.33	1	s	—	H (2)
8.37	1	d	8.9	H (13)
8.47	1	dd	8.9, 2.6	H (12)
8.69	1	d	2.6	H (10)
56.32	—	—	—	C24
102.14	—	—	—	C14
113.81	—	—	—	C13
114.74	—	—	—	C10
118.30	—	—	—	C16
123.68	—	—	—	C12
124.56	—	—	—	C18
126.31	—	—	—	C5
131.10	—	—	—	C17
136.64	—	—	—	C9
141.42	—	—	—	C4
143.66	—	—	—	C2
144.56	—	—	—	C11
156.26	—	—	—	C15

Table 2. Complete ^1H NMR and ^{13}C NMR signal assignments for compound (4).


δ (ppm)	Integration	Multiplicity	Coupling Constant (Hz)	Assignment
3.35	3	s	—	3H (22)
5.22	2	Bs	—	2H (14)
6.77	1	d	9	H (18)
6.89	1	d	2.2	H (15)

Table 2. Cont.

7.00	1	dd	9, 2,2	H (17)
7.45	1	dd	9, 2,2	H (12)
7.96–8.00	2	m	–	2H (2, 10)
8.13	1	d	9	H (13)
57.97	–	–	–	C22
102.14	–	–	–	C10
114.08	–	–	–	C15
116.12	–	–	–	C13
119.70	–	–	–	C12
124.56	–	–	–	C17
126.77	–	–	–	C19
126.92	–	–	–	C5
129.49	–	–	–	C4
134.69	–	–	–	C18
136.58	–	–	–	C9
141.96	–	–	–	C2
146.34	–	–	–	C11
156.71	–	–	–	C16

Figure 1. ¹H NMR spectrum of compound (3).

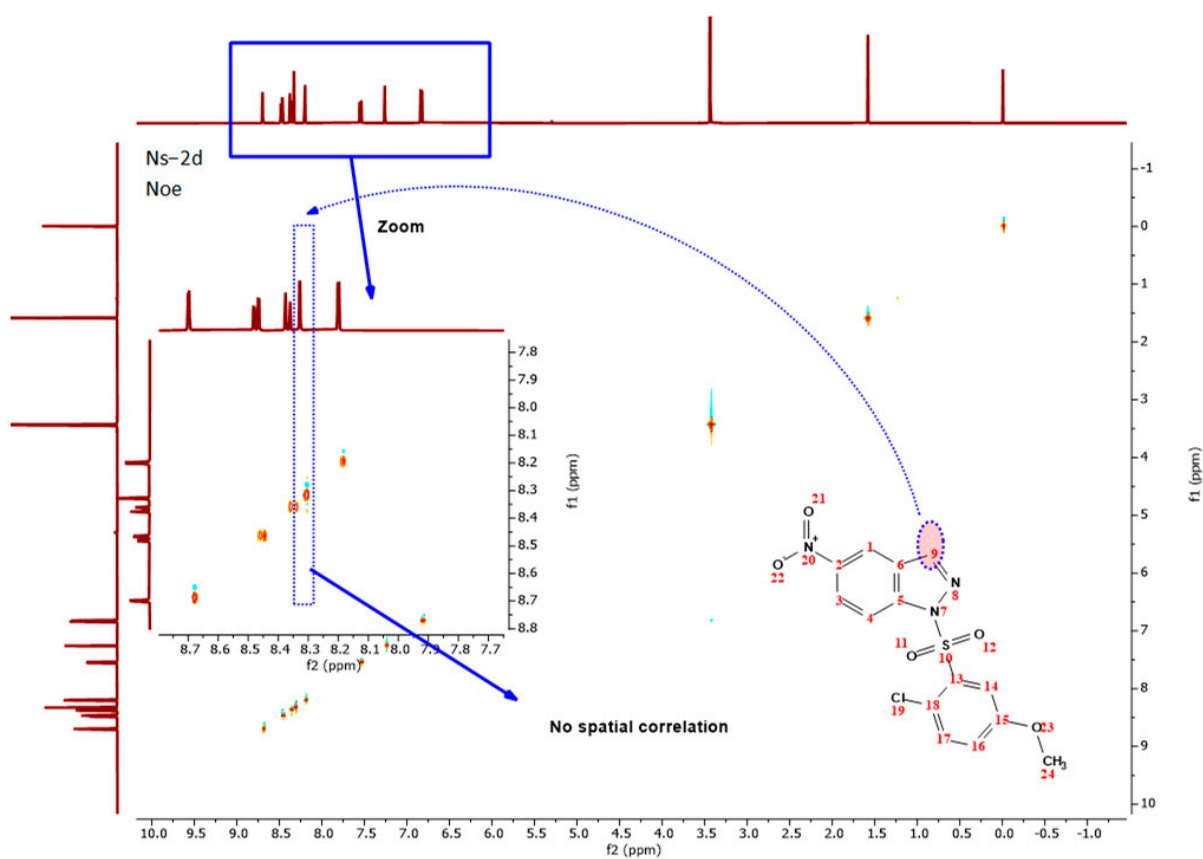
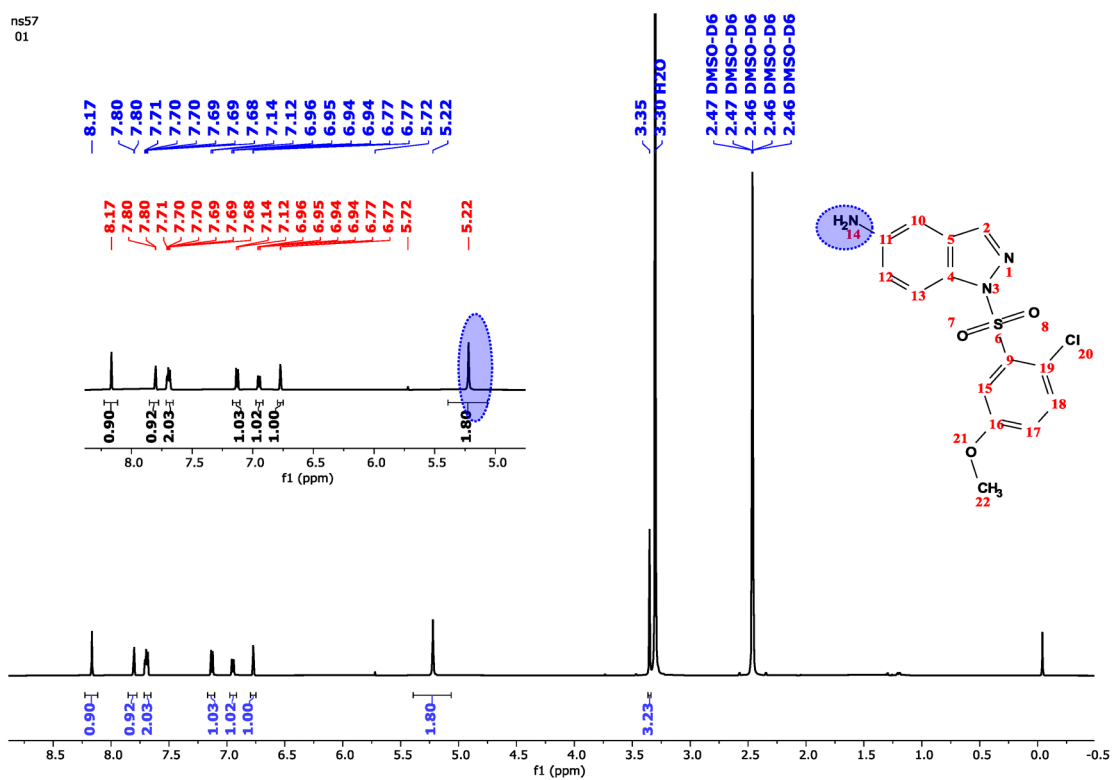


Figure 2. NOESY NMR spectrum of compound (3).

Figure 3. ¹H NMR spectrum of compound (4).

In the IR spectrum, and as illustrated in Figure 4 for compound (3), we observed that the sulfonyl group (SO_2) exhibits strong bands in 1170 cm^{-1} and 1345 cm^{-1} ($\text{S}=\text{O}$ stretch). The nitro group (NO_2), on the other hand, is characterized by bands at 1345 cm^{-1} and 1515 cm^{-1} ($\text{N}=\text{O}$ stretch). The aromatic C-H stretching vibrations are seen around 3106 cm^{-1} . The methoxy group (OCH_3), in addition, shows peaks between 2830 cm^{-1} and 2950 cm^{-1} (C-H stretch) and a strong peak around 1074 cm^{-1} (C-O stretch). On the other hand, we can see in Figure 5 that the sulfonyl group (SO_2) of the compound (4) shows strong bands at 1174 cm^{-1} and 1356 cm^{-1} ($\text{S}=\text{O}$ stretch). The amine group (NH_2) is indicated by bands around 3353 cm^{-1} and 3426 cm^{-1} ($\text{N}-\text{H}$ stretch). Aromatic C-H stretching vibrations appear around 3092 cm^{-1} . The methoxy group (OCH_3) exhibits bands between 2810 cm^{-1} and 2930 cm^{-1} (C-H stretch) and a strong peak around 1059 cm^{-1} (C-O stretch). These spectroscopic features allow us to clearly distinguish between the nitro compound (3) and the amine compound (4), demonstrating the effectiveness of NMR and IR spectroscopy in structural elucidation.

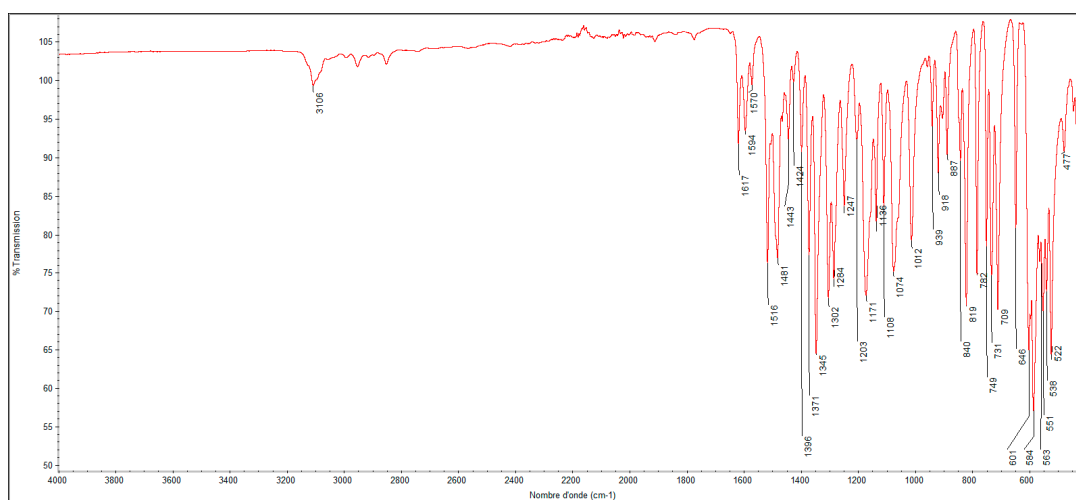


Figure 4. IR spectra of compound (3).

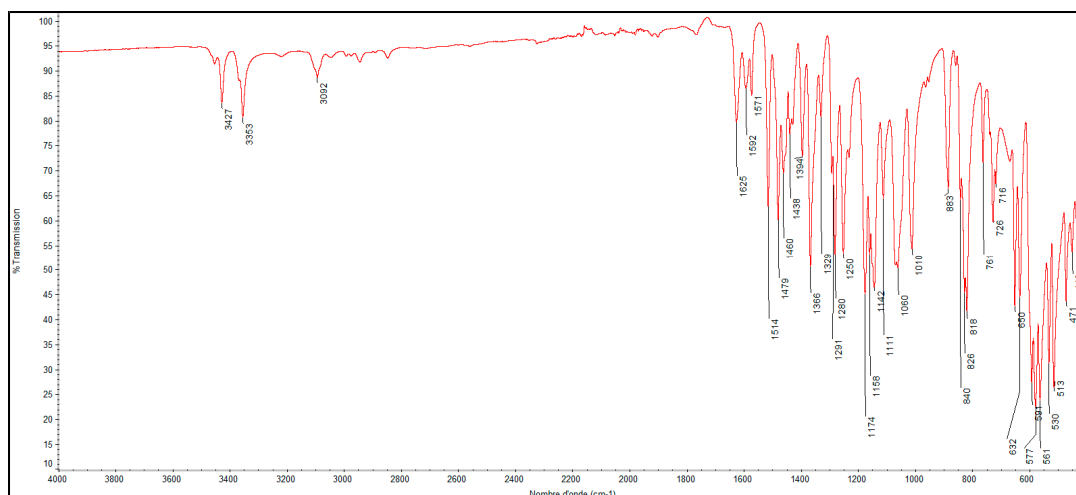


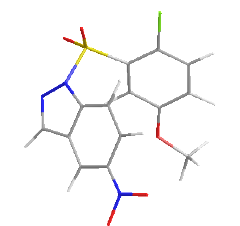
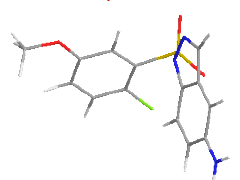
Figure 5. IR spectra of compound (4).

2.2. Molecular Docking

MAPK1 (mitogen-activated protein K=kinase 1) is a member of the MAPK (mitogen-activated protein kinase) family of serine/threonine protein kinases. This kinase is known for its crucial role in various human cancers including ovarian, colon, breast, and lung

cancers [26–29]. It has also been found to promote metastasis and invasion in gastric cancer [30]. Furthermore, the activation of MAPK1 promotes cell survival in certain tissues by inhibiting proapoptotic proteins and by stimulating anti-apoptotic factors. Inhibiting MAPK1 is therefore very important and stands as an active research area in cancer drug design and development. In this study, an *in silico* molecular docking was carried out on compounds (3) and (4) against MAPK1. As shown in Table 3, compound (3) presents good binding affinity to this kinase with a binding energy value of -7.55 Kcal/mol. Interestingly, the reduction of the nitro group of (3) to its corresponding amine (analog 4) significantly enhanced the binding affinity to the MAPK1 kinase as demonstrated by the bonding energy value of -8.34 Kcal/mol. This is probably due to the increment of the hydrogen bond donors for compound (4) as compared with compound (3). As illustrated in Figure S5, compounds (3) and (4) fit to the MAPK1 active site in a similar manner to the crystalized structure described by Aronov et al. [31]. Furthermore, the two compounds are engaged in various favorable interactions with several amino acid residues inside the MAPK1 active site as depicted in Figures 6 and 7. These results suggest that indazole derivatives (3) and (4) are promising inhibitors of the MAPK1 and could serve as good anti-cancer agents.

Table 3. Molecular docking of compounds (3) and (4).

N°	Name	Molecular Weight (g/mol)	3D Structure	B.E. (Kcal/mol)
3	1-((2-chloro-5-methoxyphenyl) sulfonyl)-5-nitro-1 <i>H</i> indazole	367.76		-7.55
4	1-((2-chloro-5-methoxyphenyl) sulfonyl)-1 <i>H</i> -indazol-5-amine	337.02		-8.34

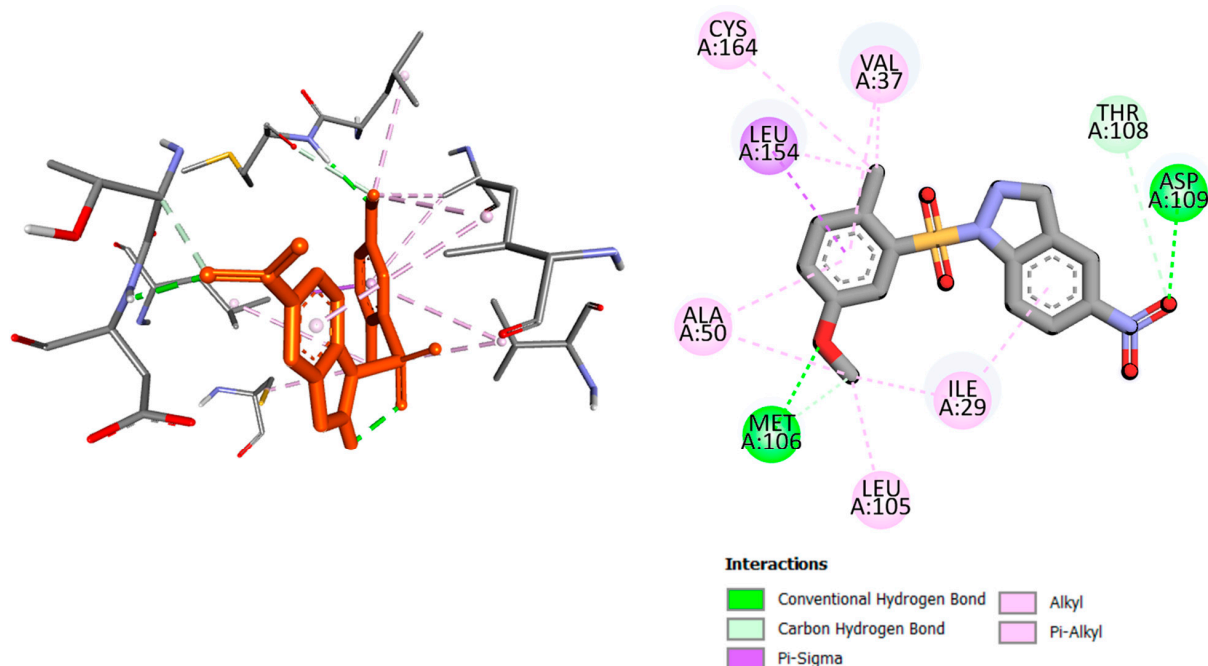


Figure 6. 3D and 2D interactions of compound (3) in the MAPK1 active site.

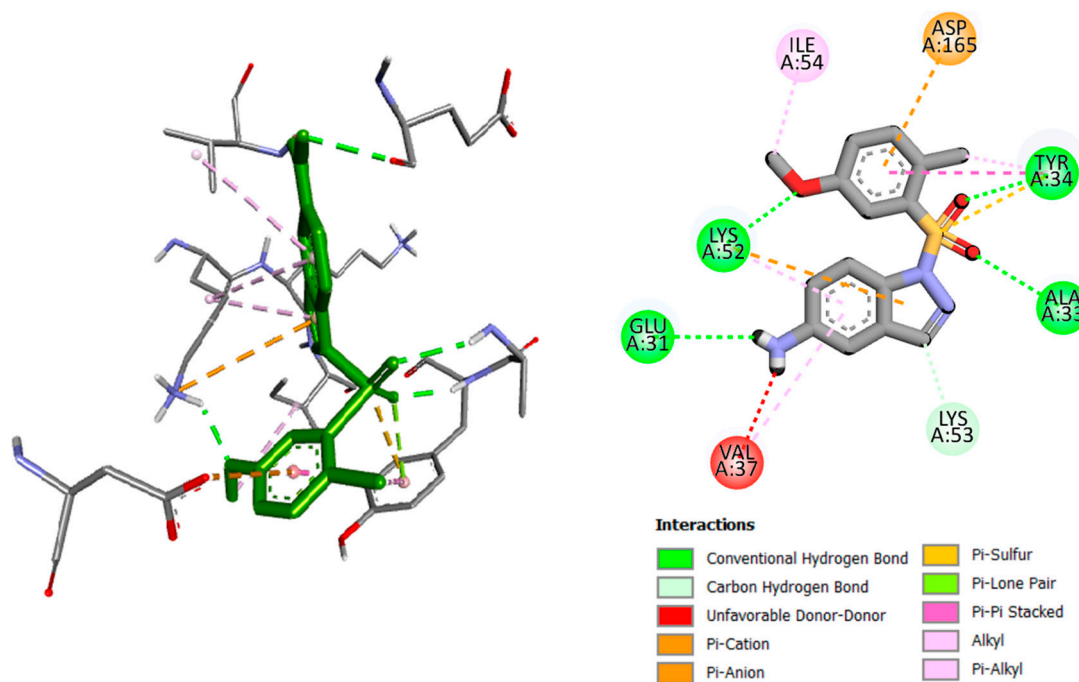


Figure 7. 3D and 2D interactions of compound (4) in the MAPK1 active site.

3. Materials and Methods

3.1. General Methods

Chemicals and reagents were obtained from commercial sources and used without further purification. Analytical thin-layer chromatography (TLC) was performed on silica gel 60 F254 (Merck Darmstadt, Germany). The compound was visualized by ultraviolet (UV) irradiation at 254 or 365 nm. Column chromatography was performed on silica gel 60 (230–400 mesh, 0.040–0.063 mm). The melting point (m.p. [°C]) was taken on samples in open capillary tubes and was not corrected using the Stuart-SMP30 apparatus (Stuart, Cincinnati, OH, USA). The infrared spectra of compounds were recorded at room temperature on a Thermo Scientific Nicolet IS50 FT-IR (Thermo scientific, Waltham, MA, USA). UV-vis spectra were recorded in the 200–800 nm range, with Spectralon as the reference, using a PerkinElmer Lambda 1050 spectrometer equipped with an integrating sphere (PerkinElmer, Shelton, CT, USA). ^1H NMR and ^{13}C NMR spectra were recorded on a Jeol 600 MHz spectrometer (Jeol, Tokyo, Japan) in an appropriate deuterated solvent at room temperature, operating at 600 MHz and 150.91 MHz. Tetramethylsilane (TMS) was used as reference. The multiplicities of the spectra are reported as follows: singlet (s), doublet (d), triplet (t), quartet (q), and multiplet (m). Coupling constants (J) are reported in hertz (Hz). High-resolution mass spectroscopy (HRMS) was performed on a Maxis Bruker 4G (Bruker, Karlsruhe, Germany).

3.2. General Synthetic Procedures

(i) To a stirred solution of 5-nitroindazole (1) (1 equivalent) in 5 mL of dry *N,N*-dimethylformamide (DMF) at 0 °C, sodium hydride (8 equivalents) was added dropwise. We obtained the sodium salt of 5-nitro-1*H*-indazole (2) intermediate, and hydrogen gas evolved. The mixture was then stirred for 30 min. Afterward, 2-chloro-5-methoxybenzene-1-sulfonyl (2 equivalents) was added, and the reaction was allowed to proceed at room temperature for 6 h. The reaction progress was monitored by thin-layer chromatography (TLC). The organic phase was extracted three times with dichloromethane (DCM) and saturated aqueous sodium chloride solution, dried over magnesium sulfate, and concentrated under reduced pressure. The crude product was purified through silica gel column chromatography to isolate the desired compound (3) in a good yield.

(ii) To a solution of compound (3) (1 equivalent) in EtOH/H₂O (3:2 (*v/v*)), NH₄Cl (5 equivalents) was added. 5 min after, zinc (3 equivalents) was added and the mixture was stirred for 3 h at room temperature. The mixture was filtered under pressure and dissolved in ethyl acetate (EtOAc). The organic phase was washed with brine, dried under magnesium sulfate, and concentrated under reduced pressure. The compound (4) was purified using column chromatography.

1-((2-chloro-5-methoxyphenyl) sulfonyl)-5-nitro-1*H*-indazole (3), white solid (yield of 88%). m.p. 204–205°. ¹H NMR (600 MHz, CDCl₃) δ 8.70 (d, *J* = 2.2, 1H), 8.47 (dd, *J* = 8.9, 2.6 Hz, 1H), 8.37 (d, *J* = 8.9 Hz, 1H), 8.33 (s, 1H), 8.20 (d, *J* = 2.2 Hz, 1H), 7.55 (dd, *J* = 8.9, 2.6 Hz, 1H), 6.83 (d, *J* = 8.9 Hz, 1H), 3.44 (s, 3H). ¹³C NMR (151 MHz, CDCl₃) δ 156.26, 144.56, 143.66, 141.42, 136.64, 131.10, 126.31, 124.56, 123.68, 118.30, 114.74, 113.81, 102.14, 56.32. IR (neat): ν 1716 (C=N), 1515 (NO, asymmetric), 1345 (NO, symmetric) cm⁻¹. HRMS [M+H]⁺ calculated for C₁₄H₁₂ClN₃O₅S: 368.0030, found: 368.0106.

1-((2-chloro-5-methoxyphenyl) sulfonyl)-1*H*-indazol-5-amine (4), white solid (yield of 92%). m.p. 194–195°. ¹H NMR (600 MHz, C₂D₆OS) δ 8.13 (s, *J* = 9 Hz, 1H), 7.96–8.00 (m, 2H), 7.45 (dd, 9.0, 2.2, 2H), 7.00 (dd, *J* = 9.0, 2.2 Hz, 1H), 6.89 (d, *J* = 2.2, 1H), 6.77 (d, *J* = 9 Hz, 1H), 5.22 (bs, 2H), 3.35 (s, 3H). ¹³C NMR (151 MHz, C₂D₆OS) δ 156.71, 146.34, 141.96, 136.58, 134.69, 129.49, 126.92, 126.77, 124.56, 119.70, 116.12, 114.08, 102.14, 56.97. IR (neat): ν 3426 (NH), 3353 (NH), 1624 (C=N) cm⁻¹. HRMS [M+H]⁺ calculated for C₁₄H₁₃ClN₃O₃S: 338.0288, found: 338.0362

3.3. Protein Retrieval and Preparation

The crystal structure of ERK2 (MAPK1) was retrieved in PDB format from the PDB databank using the PDB ID: 2OJJ. Next, the structure was prepared using BIOVIA Discovery Studio Visualizer (2021) software by removing water molecules as well as the co-crystallized ligand.

3.4. Ligands Preparation

Ligand 2D structures were sketched using Chemdraw (16.0) and then prepared by energy minimization using the MM2 algorithm within Chem 3D (16.0) software. PDBQT format was then generated using the AutoDockTools-1.5.7.

3.5. Docking

AutoDock 4.0 was used for the process of docking.

3.6. Visualization

The best pose of each ligand was then chosen for visualization and the study of the multiple interactions established between ligands and proteins using BIOVIA Discovery Studio Visualizer (2021).

3.7. NOE Experiment

The NOESY spectrum was acquired at 295 K on a JEOL NMR spectrometer operating at 600.13 MHz for ¹H, equipped with an HFX ROYAL probe. The pulse program used was noesygpphzs, a phase-sensitive gradient-enhanced NOESY with PFG zz-filter element, part of the JEOL DELTA software version 6.2. The 2D-NOESY spectrum was recorded with 2048 × 256 real points (F2, F1). Each point was acquired with 8 scans, an acquisition time of 150 ms, and an interscan delay (d1) of 1.5 s. The mixing time was set to 500 ms. The spectrum was processed to 1280 × 1024 hypercomplex points using a sepx window function.

4. Conclusions

We successfully synthesized 1-((2-chloro-5-methoxyphenyl) sulfonyl)-5-nitro-1*H*-indazole (3) through a sulfonylation reaction between 5-nitroindazole and 2-chloro-5-methoxybenzene-1-sulfonyl chloride. The reduction of the nitro group to its corresponding amine group afforded compound 1-((2-chloro-5-methoxyphenyl) sulfonyl)-1*H*-indazol-5-amine (4). The structures of

the synthesized compounds were confirmed using various spectroscopic techniques, including ^1H NMR, ^{13}C NMR, IR, and HRMS. These compounds, characterized by their specific spectral properties, add to the growing repertoire of sulfonamides, which are known for their diverse biological activities and therapeutic potentials. The good binding affinity of both compounds (3) and (4) to MAPK1 kinase demonstrated their potential as anti-cancer agents. The detailed characterization and synthesis method outlined in this study provides a robust foundation for further research and application of sulfonamide-based compounds in various biological fields.

Supplementary Materials: Figure S1: ^{13}C NMR compound 3 in CDCl_3 ; Figure S2: HRMS of compound 3; Figure S3: ^{13}C NMR compound 4 in $\text{DMSO}-d_6$; Figure S4: HRMS of compound 4; Figure S5: Superimposition of docked ligands 3 and 4 with crystalized inhibitor [31] of MAPK1.

Author Contributions: Conceptualization, S.E.K. and N.E.B.; methodology, S.E.K.; software, N.S.; validation, S.E.K. and N.E.B.; formal analysis, A.C.; investigation, N.S.; resources, S.E.K.; data curation, N.S.; writing—original draft preparation N.S. and A.C. writing—review and editing, S.E.K. and N.E.B.; visualization, S.E.K. and N.E.B.; supervision, S.E.K. and N.E.B.; project administration, S.E.K.; funding acquisition, S.E.K. All authors have read and agreed to the published version of the manuscript.

Funding: This research received no external funding.

Data Availability Statement: Data are contained within the article and Supplementary Materials.

Acknowledgments: The authors thank Euromed University of Fes for funding and for providing their facilities. N.S. and A.C. are grateful to Euromed University for the scholarship.

Conflicts of Interest: The authors declare no conflicts of interest.

References

1. Amewu, R.K.; Sakyi, P.O.; Osei-Safo, D.; Addae-Mensah, I. Synthetic and Naturally Occurring Heterocyclic Anticancer Compounds with Multiple Biological Targets. *Molecules* **2021**, *26*, 7134. [[CrossRef](#)] [[PubMed](#)]
2. Vitaku, E.; Smith, D.T.; Njardarson, J.T. Analysis of the Structural Diversity, Substitution Patterns, and Frequency of Nitrogen Heterocycles among U.S. FDA Approved Pharmaceuticals: Miniperspective. *J. Med. Chem.* **2014**, *57*, 10257–10274. [[CrossRef](#)] [[PubMed](#)]
3. Santos, A.S.; Raydan, D.; Cunha, J.C.; Viduedo, N.; Silva, A.M.S.; Marques, M.M.B. Advances in Green Catalysis for the Synthesis of Medicinally Relevant N-Heterocycles. *Catalysts* **2021**, *11*, 1108. [[CrossRef](#)]
4. Bourzikat, O.; El Abbouchi, A.; Ghammaz, H.; El Brahmi, N.; El Fahime, E.; Paris, A.; Daniellou, R.; Suzenet, F.; Guillaumet, G.; El Kazzouli, S. Synthesis, Anticancer Activities and Molecular Docking Studies of a Novel Class of 2-Phenyl-5,6,7,8-Tetrahydroimidazo [1,2-b]Pyridazine Derivatives Bearing Sulfonamides. *Molecules* **2022**, *27*, 5238. [[CrossRef](#)] [[PubMed](#)]
5. Gambouz, K.; Abbouchi, A.E.; Nassiri, S.; Suzenet, F.; Bousmina, M.; Akssira, M.; Guillaumet, G.; El Kazzouli, S. Palladium-Catalyzed Oxidative Arylation of 1 H-Indazoles with Arenes. *Eur. J. Org. Chem.* **2020**, *2020*, 7435–7439. [[CrossRef](#)]
6. Wan, Y.; He, S.; Li, W.; Tang, Z. Indazole Derivatives: Promising Anti-Tumor Agents. *ACAMC* **2019**, *18*, 1228–1234. [[CrossRef](#)]
7. Dong, J.; Zhang, Q.; Wang, Z.; Huang, G.; Li, S. Recent Advances in the Development of Indazole-based Anticancer Agents. *ChemMedChem* **2018**, *13*, 1490–1507. [[CrossRef](#)]
8. Pérez-Villanueva, J.; Yépez-Mulia, L.; González-Sánchez, I.; Palacios-Espinosa, J.; Soria-Arteche, O.; Sainz-Espuñes, T.; Cerbón, M.; Rodríguez-Villar, K.; Rodríguez-Vicente, A.; Cortés-Gines, M.; et al. Synthesis and Biological Evaluation of 2H-Indazole Derivatives: Towards Antimicrobial and Anti-Inflammatory Dual Agents. *Molecules* **2017**, *22*, 1864. [[CrossRef](#)] [[PubMed](#)]
9. Li, X.; Chu, S.; Feher, V.A.; Khalili, M.; Nie, Z.; Margosiak, S.; Nikulin, V.; Levin, J.; Sprankle, K.G.; Tedder, M.E.; et al. Structure-Based Design, Synthesis, and Antimicrobial Activity of Indazole-Derived SAH/MTA Nucleosidase Inhibitors. *J. Med. Chem.* **2003**, *46*, 5663–5673. [[CrossRef](#)]
10. Kim, S.-H.; Markovitz, B.; Trovato, R.; Murphy, B.R.; Austin, H.; Willardsen, A.J.; Baichwal, V.; Morham, S.; Bajji, A. Discovery of a New HIV-1 Inhibitor Scaffold and Synthesis of Potential Prodrugs of Indazoles. *Bioorg. Med. Chem. Lett.* **2013**, *23*, 2888–2892. [[CrossRef](#)]
11. Degnan, A.P.; Tora, G.O.; Huang, H.; Conlon, D.A.; Davis, C.D.; Hanumegowda, U.M.; Hou, X.; Hsiao, Y.; Hu, J.; Krause, R.; et al. Discovery of Indazoles as Potent, Orally Active Dual Neurokinin 1 Receptor Antagonists and Serotonin Transporter Inhibitors for the Treatment of Depression. *ACS Chem. Neurosci.* **2016**, *7*, 1635–1640. [[CrossRef](#)] [[PubMed](#)]
12. Tan, C.; Yang, S.-J.; Zhao, D.-H.; Li, J.; Yin, L.-Q. Antihypertensive Activity of Indole and Indazole Analogues: A Review. *Arab. J. Chem.* **2022**, *15*, 103756. [[CrossRef](#)]
13. Shang, C.; Hou, Y.; Meng, T.; Shi, M.; Cui, G. The Anticancer Activity of Indazole Compounds: A Mini Review. *Curr. Top. Med. Chem.* **2021**, *21*, 363–376. [[CrossRef](#)]

14. López-Vallejo, F.; Castillo, R.; Yépez-Mulia, L.; Medina-Franco, J.L. Benzotriazoles and Indazoles Are Scaffolds with Biological Activity against *Entamoeba Histolytica*. *SLAS Discov.* **2011**, *16*, 862–868. [[CrossRef](#)]
15. Tzvetkov, N.T.; Hinz, S.; Küppers, P.; Gastreich, M.; Müller, C.E. Indazole- and Indole-5-Carboxamides: Selective and Reversible Monoamine Oxidase B Inhibitors with Subnanomolar Potency. *J. Med. Chem.* **2014**, *57*, 6679–6703. [[CrossRef](#)]
16. El Abbouchi, A.; El Brahmi, N.; Hiebel, M.-A.; Bignon, J.; Guillaumet, G.; Suzenet, F.; El Kazzouli, S. Synthesis and Biological Evaluation of Ethacrynic Acid Derivatives Bearing Sulfonamides as Potent Anti-Cancer Agents. *Bioorg. Med. Chem. Lett.* **2020**, *30*, 127426. [[CrossRef](#)] [[PubMed](#)]
17. Boztaş, M.; Çetinkaya, Y.; Topal, M.; Gülçin, İ.; Menzek, A.; Şahin, E.; Tanc, M.; Supuran, C.T. Synthesis and Carbonic Anhydrase Isoenzymes I, II, IX, and XII Inhibitory Effects of Dimethoxybromophenol Derivatives Incorporating Cyclopropane Moieties. *J. Med. Chem.* **2015**, *58*, 640–650. [[CrossRef](#)] [[PubMed](#)]
18. Ballatore, C.; Huryn, D.M.; Smith, A.B. Carboxylic Acid (Bio)Isosteres in Drug Design. *ChemMedChem* **2013**, *8*, 385–395. [[CrossRef](#)]
19. Cao, X.; Sun, Z.; Cao, Y.; Wang, R.; Cai, T.; Chu, W.; Hu, W.; Yang, Y. Design, Synthesis, and Structure–Activity Relationship Studies of Novel Fused Heterocycles-Linked Triazoles with Good Activity and Water Solubility. *J. Med. Chem.* **2014**, *57*, 3687–3706. [[CrossRef](#)]
20. Feng, Z.; Lu, X.; Gan, L.; Zhang, Q.; Lin, L. Xanthones, a Promising Anti-Inflammatory Scaffold: Structure, Activity, and Drug Likeness Analysis. *Molecules* **2020**, *25*, 598. [[CrossRef](#)]
21. Gao, F.; Wang, T.; Xiao, J.; Huang, G. Antibacterial Activity Study of 1,2,4-Triazole Derivatives. *Eur. J. Med. Chem.* **2019**, *173*, 274–281. [[CrossRef](#)] [[PubMed](#)]
22. Scozzafava, A.; Owa, T.; Mastrolorenzo, A.; Supuran, C. Anticancer and Antiviral Sulfonamides. *Curr. Med. Chem.* **2003**, *10*, 925–953. [[CrossRef](#)]
23. Rodés, B.; Sheldon, J.; Toro, C.; Jiménez, V.; Álvarez, M.Á.; Soriano, V. Susceptibility to Protease Inhibitors in HIV-2 Primary Isolates from Patients Failing Antiretroviral Therapy. *J. Antimicrob. Chemother.* **2006**, *57*, 709–713. [[CrossRef](#)]
24. Gao, F.; Zhang, X.; Wang, T.; Xiao, J. Quinolone Hybrids and Their Anti-Cancer Activities: An Overview. *Eur. J. Med. Chem.* **2019**, *165*, 59–79. [[CrossRef](#)] [[PubMed](#)]
25. Wan, Y.; Long, J.; Gao, H.; Tang, Z. 2-Aminothiazole: A Privileged Scaffold for the Discovery of Anti-Cancer Agents. *Eur. J. Med. Chem.* **2021**, *210*, 112953. [[CrossRef](#)] [[PubMed](#)]
26. Hong, L.; Wang, Y.; Chen, W.; Yang, S. MicroRNA-508 Suppresses Epithelial-Mesenchymal Transition, Migration, and Invasion of Ovarian Cancer Cells through the MAPK1/ERK Signaling Pathway. *J. Cell. Biochem.* **2018**, *119*, 7431–7440. [[CrossRef](#)]
27. Wang, M.; Liao, Q.; Zou, P. PRKCZ-AS1 Promotes the Tumorigenesis of Lung Adenocarcinoma via Sponging miR-766-5p to Modulate MAPK1. *Cancer Biol. Ther.* **2020**, *21*, 364–371. [[CrossRef](#)]
28. Hamadneh, L.; Bahader, M.; Abuarqoub, R.; AlWahsh, M.; Alhusban, A.; Hikmat, S. PI3K/AKT and MAPK1 Molecular Changes Preceding Matrix Metalloproteinases Overexpression during Tamoxifen-Resistance Development Are Correlated to Poor Prognosis in Breast Cancer Patients. *Breast Cancer* **2021**, *28*, 1358–1366. [[CrossRef](#)]
29. Guo, Y.J.; Pan, W.W.; Liu, S.B.; Shen, Z.F.; Xu, Y.; Hu, L.L. ERK/MAPK signalling pathway and tumorigenesis. *Exp. Ther. Med.* **2020**, *19*, 1997–2007. [[CrossRef](#)]
30. Wang, Y.; Guo, Z.; Tian, Y.; Cong, L.; Zheng, Y.; Wu, Z.; Shan, G.; Xia, Y.; Zhu, Y.; Li, X.; et al. MAPK1 Promotes the Metastasis and Invasion of Gastric Cancer as a Bidirectional Transcription Factor. *BMC Cancer* **2023**, *23*, 959. [[CrossRef](#)]
31. Aronov, A.M.; Baker, C.; Bemis, G.W.; Cao, J.; Chen, G.; Ford, P.J.; Germann, U.A.; Green, J.; Hale, M.R.; Jacobs, M.; et al. Flipped out: Structure-Guided Design of Selective Pyrazolopyrrole ERK Inhibitors. *J. Med. Chem.* **2007**, *50*, 1280–1287. [[CrossRef](#)] [[PubMed](#)]

Disclaimer/Publisher’s Note: The statements, opinions and data contained in all publications are solely those of the individual author(s) and contributor(s) and not of MDPI and/or the editor(s). MDPI and/or the editor(s) disclaim responsibility for any injury to people or property resulting from any ideas, methods, instructions or products referred to in the content.